Phase Transition of the PLGA-*g*-PEG Copolymer Aqueous Solutions

Byeongmoon Jeong,*,† Charles F. Windisch, Jr.,‡ Moon Jeong Park,§ Youn Soo Sohn,† Anna Gutowska,‡ and Kookheon Char§

Department of Chemistry, Division of Nano Science, Ewha Womans University, Daehyun-Dong, Seodaemun-Ku, Seoul, 120-750, Korea, Pacific Northwest National Lab. (PNNL), 902 Battelle Boulevard, P.O. Box 999, K2-44, Richland, Washington 99352, and Polymer Thin Films Laboratory, School of Chemical Engineering, Seoul National University, Seoul 151-744, Korea

Received: October 29, 2002; In Final Form: June 7, 2003

The aqueous solution of poly(lactic acid-*co*-glycolic acid)-*g*-poly(ethylene glycol) becomes a gel as the temperature increases. The sol-to-gel transition temperature can be controlled from 15 to 45 °C by varying the number of poly(ethylene glycol) grafts and the composition of the polymer. In addition, hysteresis between heating and cooling cycles could be controlled by adding poly(ethylene glycol) with different molecular weights as an additive. To prove the hypothesis of micellar aggregation for the sol-to-gel transition and the change in hydration status for the gel-to-sol transition, several experiments were performed. Small-angle neutron scattering and Raman spectroscopy sensitively detected the sol-to-gel transition, because it involves aggregation of the scattering particle of micelles. IR and ^{13}C NMR showed that little change in hydration status is involved during the sol-to-gel transition, whereas significant change in hydration status is involved in the gel-to-sol transition. The intrinsic viscosity of the PEG showed that more significant dehydration can occur when PEG is attached to the hydrophobic group. On the basis of the experiments above, PEG dehydration is the major driving force for the phase change of the PLGA-*g*-PEG aqueous solution. At the sol-to-gel transition temperature, partial dehydration of the PEG induces the micellar aggregation while keeping the core−shell structure. However, at the gel-to-sol transition, dehydration of the PEG is so significant that the core−shell structure is broken and macroscopic phase separation occurs. These phenomena were associated with changes in the carbonyl stretching and ether bending modes in the IR spectra.

I. Introduction

There has been extensive research on stimuli sensitive polymers which undergo large conformational changes in response to temperature, pH, light, electric field, chemicals, and so forth.[1−7] The sol-to-gel transition of polymer aqueous solutions driven by a change in temperature has been a special concern because organic solvent-free injectable systems for drug delivery and tissue engineering can be designed.[8−10] Such a system enables pharmaceutical agents to be easily entrapped and form a depot by simple syringe injection at a target site, avoiding surgical procedure. Typical examples of aqueous thermogelling systems are poly(N-isopropyl acryl amide) copolymers, poly(ethylene glycol)/poly(propylene glycol) block copolymers (Poloxamers), poly(ethylene glycol)/poly(butylenes glycol) block copolymers, and Poloxamer-*g*-poly(acrylic acid) (Smart gel).[11−14] In the search for biodegradable thermogelling materials for biomedical applications, a series of poly(ethylene glycol)/poly(lactic acid-*co*-glycolic acid) (PEG/PLGA) triblock and graft copolymers and poly(ethylene glycol)/poly(propylene furmarate) (PEG/PPF), chitosan/glycerol phosphate, and polyphosphazene/PEG/oligopeptide have been developed. They are reported to be very promising biomaterials for drug delivery and tissue engineering.[15−19]

The copolymers consisting of the hydrophobic PLGA block and the hydrophilic PEG block form a core−shell structure in water.[14−16,20] Cryo-transmission electron microscope (Cryo-TEM) imaging showed the micellar structure in water. The increase in the absorbance at 356 nm of the hydrophobic dye, 1,6-diphenyl-1,3,5-hexatriene, indicates hydrophobic domain formation above its critical concentration in water. ^{13}C NMR shows a sharp PEG peak and a collapsed PLGA peak in D_2O which is a good solvent for PEG but a poor solvent for PLGA. In constrast, both PEG and PLGA appear as sharp peaks in $CDCl_3$ which is a good solvent for both PEG and PLGA. The sharp PEG peak and collapsed PLGA peak in the sol state, at the sol-to-gel transition temperature and through the gel phase, indicate a core−shell structure of the gel. Above the syneresis temperature, the PLGA peak increased and sharpened, indicating an increase in the dynamic motion of PLGA, and the macroscopic phase separation (syneresis) was observed, suggesting that the core−shell structure is broken.

In this paper, as a continuation of research on thermogelling PEG/PLGA system, poly(lactic acid-*co*-glycolic acid)-*g*-poly(ethylene glycol) (PLGA-*g*-PEG) was investigated to answer several questions: (1) Does the change in the number of the PEG graft and composition affect the sol−gel transition temperature? (2) Does the PEG affect the aggregation of the polymers, resulting in the change in sol−gel transition temperature or hysteresis loop between heating and cooling cycle? (3) Is the basic structure of micelles preserved during the sol-to-gel transition (lower transition) of the PLGA-*g*-PEG copolymer aqueous solution, indicating little or no change in hydration

* To whom correspondence should be addressed. E-mail: bjeong@ewha.ac.kr; fax: 82-2-3277-3411; tel: 82-2-3277-2384.
† Ewha Womans University.
‡ Pacific Northwest National Lab.
§ Seoul National University.

10.1021/jp027339n CCC: $25.00
Published on Web 08/22/2003

status of the polymer? On the other hand, a large change in aggregation status will lead to an increase in viscosity or modulus. Such a change in aggregation status can be detected by scattering instruments such as Raman spectroscopy and small-angle neutron scattering (SANS). The gel-to-sol transition (upper transition) of the PLGA-*g*-PEG copolymer aqueous solution accompanies the macroscopic phase separation between water and polymer. (4) Can such a significant change in hydration status during gel-to-sol transition be detected by infrared (IR) absorption spectroscopy? IR spectra may also give a clue whether PEG or PLGA is more responsible for dehydration mechanism. The PEG is known to be dehydrated with increasing temperature.[21] Such a change should be reflected in the intrinsic viscosity of the PEG. (5) Does the methoxy terminated PEG show different behavior compared with a regular PEG with dihydroxyl groups?

To answer the above questions, we synthesized several PLGA-*g*-PEG polymers and investigated the PLGA-*g*-PEG aqueous solution using the various instrumental methods discussed above.

II. Experimental Section

Materials. DL-lactide (Polyscience) and glycolide (Polyscience) were recrystallized in ethyl acetate. Stannous octoate (Aldrich), epoxy terminated poly(ethylene glycol) (EPEG) (MW ~ 600 and 1000 Polyscience), monomethoxy poly(ethylene glycol) MPEG (MW = 550, Aldrich), and PEG (600, Union Carbide) were used as received.

Synthesis. The PLGA-*g*-PEG was prepared by direct polymerization of DL-lactide, glycolide, and EPEG at 130 °C for 24 h, using stannous octoate as a catalyst. The detailed procedure was reported elsewhere.[20,22] Toluene was used as a solvent. Initially, half of the toluene was distilled off to remove residual water in the EPEG, and then DL-lactide, glycolide, and stannous octoate were added into the reaction mixture. The graft copolymers were precipitated into excess ethyl ether and residual solvent was removed under vacuum.

Gel Permeation Chromatography (GPC). The GPC system (Waters 515), with a refractive index detector (Waters 410) and a light-scattering detector in series, was used to obtain absolute molecular weight and molecular weight distributions.[23] Styragel HMW 6E and HR 4E columns (Waters) were used in series. Tetrahydrofuran (THF) was used as an eluting solvent.

Sol−Gel Transition. The sol−gel transition was determined by a test tube inverting method and dynamic mechanical analysis. The aqueous polymer solutions of each concentration were prepared by dissolving the PLGA-*g*-PEG in deionized water at 4 °C for 12 h. For the test tube inverting method, the 4-mL vials (diameter 1.1 cm) containing 0.5 mL of polymer solutions were immersed in a water bath at a designated temperature for 15 min. The transition temperatures were determined by flow (sol)−no flow (gel) criterion when the vial was inverted using a temperature increment of 1 °C per step.[24,25] The accuracy of the sol−gel transition temperature was ±1 °C.

In dynamic mechanical analysis (Rheometric Scientific: SR 2000), the polymer solution was placed between parallel plates having a diameter of 25 mm and a gap distance of 0.5 mm. The data were collected under controlled stress (4.0 dyn/cm^2) and a frequency of 1.0 rad/second.[26] The heating rate was 0.2 °C/min.

NMR Study. NMR spectrometer (Varian VXR 300) was used for ^{1}H NMR to study composition of the polymer.

Intrinsic Viscosity. Using a Cannon−Fenske viscometer (KIMAX size 50, A65), intrinsic viscosity ([η]) of PEG in water was determined by eq 1. *y*-intercept in reduced viscosity (η_{red}) versus concentration (*c*) gives intrinsic viscosity at that temperature.

$$\eta_{red} = (t/t_0 - 1)/c = [\eta] + k[\eta]^2 c \quad (1)$$

The upper limit of solution concentration (*C**, overlap concentration) in viscosity measurement is given by eq 2

$$C^* = K/[\eta] \quad (2)$$

where *C** is the concentration at which the polymer coils are just touching together and *K* is a constant of the order of unity. In this experiment, the concentrations of polymer were chosen where *C*[η] is lower than 0.25.[27] The concentration ranged from 0.5 to 6 g/dl for PEG 600 or MPEG 550.

TABLE 1: List of the PLGA-*g*-PEG Copolymer

	number average molecular weight[a] (M_n)	PDI[a,b]	composition[c] (DDLA/GA/EG)	number of PEG graft per PLGA backbone[d] (G_n)
PI	6000	1.7	1.21/0.37/1.0	3
PII	7800	1.4	1.20/0.38/1.0	4
PIII	9300	1.5	1.14/0.36/1.0	5
PIV	10 000	2.0	0.78/0.25/1.0	4

[a] Determined by GPC. [b] Polydispersity index. [c] Determined by ^{1}H NMR in $CDCl_3$ based on ethylene glycol (4H. 3.6 ppm), lactic acid (3H, 1.5 ppm), and glycolic acid (2H, 4.8 ppm) moieties of the polymers. [d] Number of graft (G_n) was calculated from molecular weight and composition on the basis of PEG molecular weight. As the first-order approximation, M_n and G_n are given by the following equations: $M_n \sim 72x + 58y + 44z'$, $G_n = 44z'/600$ for PI, PII, PIII; $G_n = 44z'/1000$ for PIV. $z' = G_n m$. *x*, *y*, *z*′, G_n, and *m* are the number of repeating units of lactic acid, glycolic acid, ethylene glycol, number of PEG graft per PLGA backbone, and number of repeating units in each PEG graft, respectively, and the mole ratio of *x*/*y*/*z*′ is given by the fourth column of the table.

Infrared (IR) Spectroscopy. Aqueous polymer solutions (25 wt % of PIII in Table 1) were loaded in a temperature-controlled IR Cell (Willmad) and the IR spectra (Nicolette: Magna IR 860 Spectrometer) were recorded with increasing temperature in the range of 12~50 °C. The designated temperature was maintained for 30 min. The resolution of the peak was fixed at 1 cm^{-1}. The IR spectra of neat polymer (PIII in Table 1) cast without water was recorded as a reference in the same temperature range.

Raman Spectroscopy. Raman spectra were acquired for aqueous polymer solution (25 wt % of PIII in Table 1) in quartz cuvettes using a backscattering configuration and a Spex (Edison, NJ) Model 1877 Triple spectrometer. The 488.0-nm line of a Coherent (Santa Clara, CA) Innova 307 Argon Ion Laser was used for excitation and the detector was a Princeton Instruments (Trenton, NJ) LN/CCD detector. The slit width was 400 μm and the exposure time was 1000 s. Spectral analysis was performed using Galactic Industries (Salem, NH) Grams 386 software. All spectra were corrected for contribution from the quartz container. Estimated uncertainty of the peak frequencies was ±1 cm^{-1}.

Small-Angle Neutron Scattering (SANS). Small-angle neutron scattering experiments were performed using an 8-m SANS facility at the Korea Atomic Energy Research Institute (KAERI) equipped with two-dimensional position-sensitive detector. The sample-to-detector distance of 4.6 m and a neutron beam of 5.1 Å wavelength were used to yield scattering vectors $\mathbf{q} = (4\pi/\lambda)\sin(\theta/2)$ in the range of 0.07~1.0 nm^{-1} and the neutron beam has a wavelength resolution ($\Delta\lambda/\lambda$) of 10%. A beam stopper with a diameter of 55 mm was placed in front of

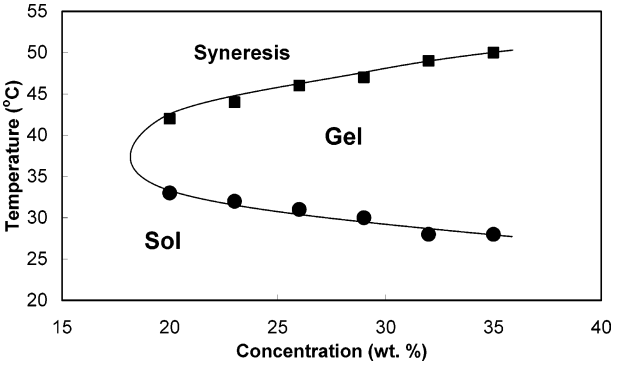

Figure 1. Phase diagram of the PLGA-*g*-PEG (PIII) aqueous solutions. Filled circles and squares indicate sol-to-gel transition and gel-to-sol transition, respectively.

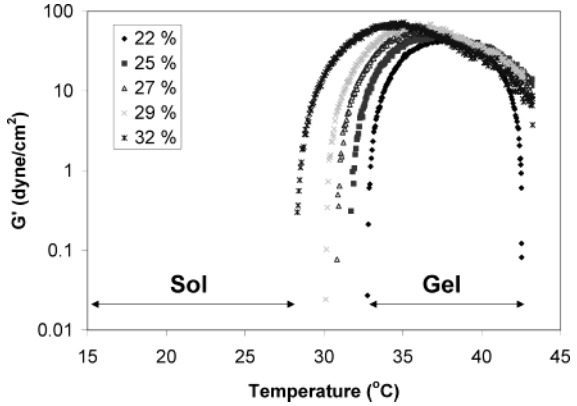

Figure 2. Storage modulus (G′) of the PLGA-*g*-PEG (PIII) aqueous solution as a function of temperature. Heating rate was 0.2 °C/min. The legends are concentrations of polymers in water. Abrupt increase in G′ is an indication of the sol-to-gel transition.

the detector to prevent the damage of the detector center from exposure to the direct neutron beam. For temperature control, a circulating bath in the range of 0−100 °C with an accuracy of ±0.01 °C was employed. Deuterium oxide (D_2O, 99.9 atom % D) purchased from Aldrich Chemical was used to obtain good contrast and low background for the neutron-scattering experiments. The copolymer was dissolved at room temperature with 100% D_2O and the samples were placed between two sealed quartz windows with a flight path of 2 mm after filtering the samples with filters of 0.45-μm pore size. All the measurements were taken after 30 min of equilibration time and all the scattering data obtained were corrected for sample transmission, incident wavelength distribution, and background originating from quartz cells filled with D_2O. The resulting one-dimensional scattering data calibrated using a well-characterized silica standard are the differential scattering cross section, $d\Sigma/d\Omega$, as a function of **q** in absolute units of cm^{-1}.

III. Results and Discussion

Synthesis. The PLGA-*g*-PEG was synthesized by one-step polymerization of DL-lactide, glycolide, and epoxy terminated poly(ethylene glycol) in the presence of stannous octoate as a catalyst. This procedure does not require a strict anhydrous condition of the PEG−PLGA−PEG triblock copolymer synthesis. ^{1}H NMR spectra show an ethylene glycol unit at 3.6 ppm, a lactic acid unit at 5.3 ppm (methine) and 1.8 ppm (methyl), and a glycolic acid unit at 4.8 ppm.[28] Absolute number average molecular weight (M_n) and polydispersity index (PDI) of the PLGA-*g*-PEG determined by the GPC were in a range of 6000∼10 000 and 1.4∼2.0, respectively. On the basis of this composition of the PLGA-*g*-PEG copolymers calculated by ^{1}H NMR and absolute molecular weight of graft copolymers, the number of the PEG grafts is calculated to be in a range of 3∼5.[20] Table 1 summarizes the polymers investigated in this study.

Sol−Gel Transition. The phase diagram of the PEG-*g*-PLGA (PIII) aqueous solutions determined by a test tube inverting method is shown in Figure 1. The sol-to-gel transition was accompanied by a sharp increase in viscosity as would be discussed in rheological study. The sol-to-gel transition involving aggregation of micelles[20] increases the scattering of light and was sensitively detected by scattering instruments discussed later. The critical gel concentration (CGC) above which gel phase appears was about 18 wt %. The transparent gel became turbid as the temperature increased, indicating more aggregations occurred between 35 and 45 °C. Further increase in temperature resulted in syneresis of the gel, and the system flows by gel-to-sol transition which is marked as squares in Figure 1. At this temperature, a macromolecular phase separation, syneresis, between the polymer and water occurred and some water was exuded from the gel phase while the gel began to flow because of lack of rigidity and increase in thermal energy.

Such a gel-to-sol transition involving dehydration was sensitively detected by IR spectroscopy discussed later. The upper sol is a two-phase sol at the temperature above the gel-to-sol transition, whereas a one-phase sol exists at the temperature below the sol-to-gel transition as shown in the phase diagram in Figure 1.

Rheological Study. The storage modulus (G′) of the aqueous solution of the PLGA-*g*-PEG begins to increase upon sol-to-gel transition (Figure 2). The modulus in sol state was less than 0.01 dyn/cm^2 and was not recorded in this rheometer. The modulus increased in a very abrupt manner by the sol-to-gel transition, which indicates that the sol-to-gel transition is a cooperated mechanism rather than sequential mechanism. The sol-to-gel transition temperature varied over 33 to 27 °C by varying the concentration from 22 to 32 wt %. The decrease in the G′ above 43 °C indicates the gel-to-sol transition at higher temperature. The presence of the gel phase around body temperature (37 °C) indicates that the material is a promising candidate for an injectable depot system that can be formulated at room temperature or lower and forms a gel depot in situ upon subcutaneous or intramuscular injection. The pharmaceutical agents would then be slowly released from the in situ formed gel.

The real part (η') of complex viscosity was recorded as a function of temperature in Figure 3. η' increased with gelation and reached a plateau value similar to the storage modulus. η' increased about 1000 times because of the sol-to-gel transition.

The storage modulus (G′) is a measure of the load-bearing capacity of a material when cyclic deformation is applied. In the glassy state of typical polymer, storage moduli of polymers are an order of 10^{10} dyn/cm^2.[29] In drug delivery application, a hydrogel is defined as three-dimensional mass holding an equilibrium amount of water without being dissolved out in the excess amount of water. The PLGA-*g*-PEG keeps its integrity more than three months in vivo as well as in vitro, indicating a hydrogel system.[7,16] The exact determination of the sol-to-gel transition temperature is a controversial issue. Several methods have been reported such as test tube tilting method, falling ball method, and dynamic mechanical analysis. In PLGA-*g*-PEG system, the three methods gave practically the same temperature in a range of ±1 °C when the abrupt increase in G′ was used for the determination of the sol-to-gel transition.[20] The sol-to-gel transition temperature was estimated by extrapolating the

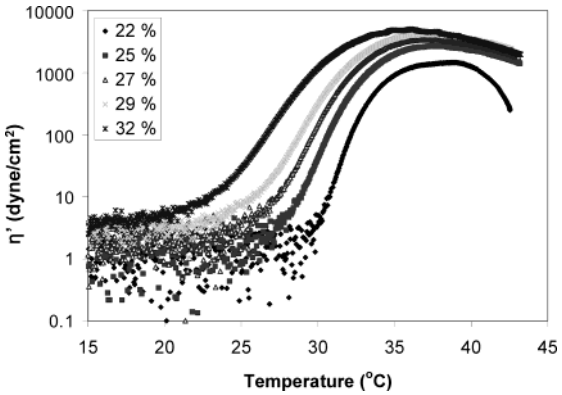

Figure 3. Real part (η') of complex viscosity of the PLGA-*g*-PEG (PIII) aqueous solution as a function of temperature. Heating rate was 0.2 °C/min. The legends are concentrations of polymers in water. Abrupt increase in η' is an indication of the sol-to-gel transition.

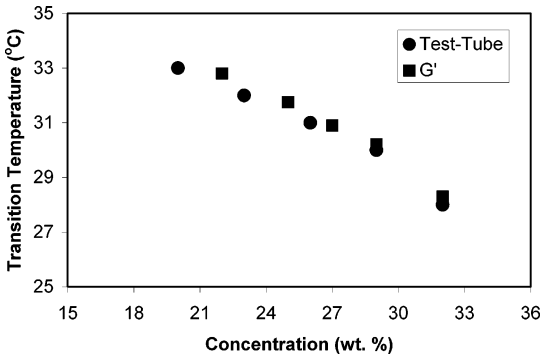

Figure 4. Comparison of sol-to-gel transition temperatures of the PLGA-*g*-PEG (PIII) determined by test tube inverting method (filled circle) and G′ from dynamic mechanical analysis (filled square). It shows consistency of both methods.

near vertical portion of the G′ curves (Figure 2) to the temperature axis. The sol-to-gel transition temperatures determined by the G′-temperature curve correlated well with those determined by test tube inverting method (Figure 4).

The control of the sol−gel transition temperature is very important in designing an injectable depot system because it determines the formulation temperature and injectability. The amount of initial burst release of the incorporated drug is also related to the sol-to-gel transition temperature. The lower the sol-to-gel transition temperature, the faster the gelation at 37 °C when the depot system is prepared in situ. This decreases the initial burst of incorporated drug. The sol-to-gel transition temperature was controlled from 15 to 45 °C by varying polymer composition, number of the PEG graft, and PEG molecular weight (Figure 5). The more hydrophilic the polymer prepared by higher PEG content or longer PEG length, the higher the sol-to-gel transition of the polymer aqueous solution. The increase in η' (Figure 5a) and G′ (Figure 5b) are caused by the sol-to-gel transition as discussed before.

The PEG affected the sol-to-gel transition of the PLGA-*g*-PEG (III) aqueous solution (Figure 6). By increasing the molecular weight of the PEG, the total PEG content by weight increases at a fixed 1.0 mole percent of the PEG relative to the PLGA-*g*-PEG copolymers. As the molecular weight of PEG increased, the viscosity of the gel decreased. The cell growth depends on the stiffness or modulus of the hydrogel as in the case of smooth muscle cell and NIH 3T3 cell.[30,31] Therefore, the stiffness control of the hydrogel is important in cell delivery system. By adding the PEG, the stiffness can be optimized in thermogelling system. The other important finding was that the

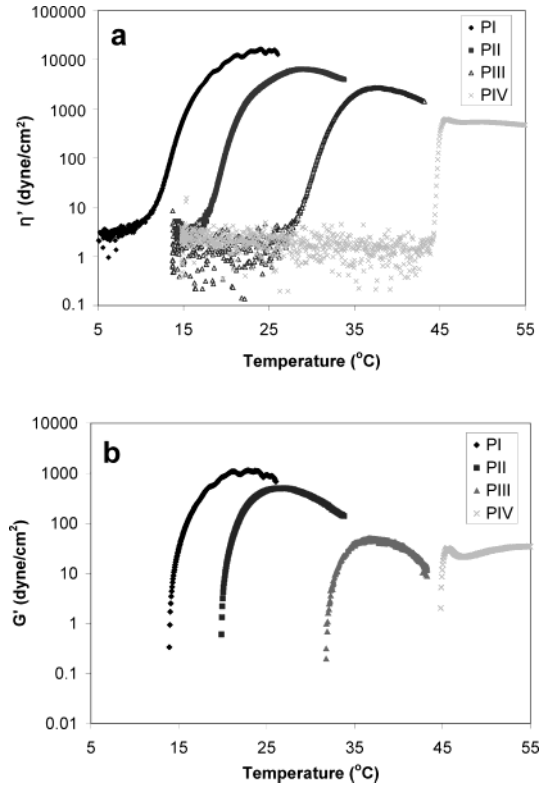

Figure 5. Effect of polymer composition on the sol−gel transition of the PLGA-*g*-PEG aqueous solution. The abrupt increases in real part of complex viscosity (η')(a) and real part of modulus (G′) (b) indicate the sol-to-gel transition. The legends are polymers listed in Table 1. The sol-to-gel transition temperature could be controlled from 15 to 45 °C.

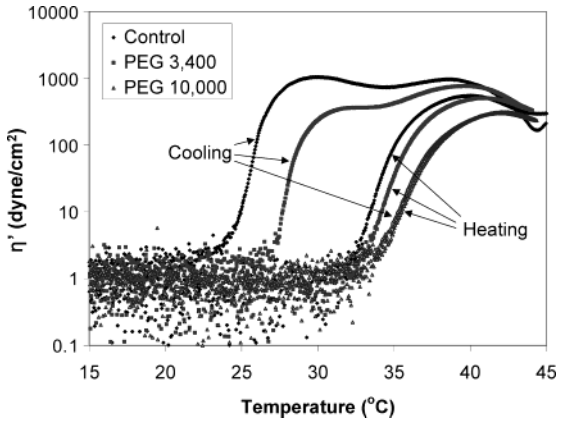

Figure 6. Effect of PEG additives on the sol−gel transition of the PLGA-*g*-PEG copolymer (PIII) aqueous solution (23 wt %). The abrupt increase in real part (η') of complex viscosity indicates the sol-to-gel transition. Control is the PLGA-*g*-PEG aqueous solution with no external PEG additives. PEG 3400 and PEG 10 000 are the PLGA-*g*-PEG aqueous solutions with the PEG additives (1 mol %). The numbers, 3400 and 10 000, are the molecular weights of the PEG used as additives.

hysteresis loop between heating and cooling curves could be controlled by the PEG. The system becomes more hydrophilic by adding the PEG, resulting in acceleration of the kinetics of water sorption by the hydrogel. Therefore, hysteresis of the sol-to-gel and gel-to-sol transition decreases with increasing the amount of PEG. The sol-to-gel transition temperature, gel viscosity (or modulus), and a hysteresis loop could be controlled by adding the PEG with an optimal molecular weight. This fact also suggests that the reconstitution of a drug formulation using this polymer can be improved by adding the PEG. One of the

TABLE 2: Viscosity−Molecular Weight Relationship of the PEG[c]

temperature (°C)	K (dl/g)	a	molecular weight range[a]	calculated [η] (dl/g)[b]	measured [η] PEG 600	measured [η] MPEG 550
20	$[\eta] = 0.02 + 0.00016\ M^{0.76}$		60∼11 000	0.0407	0.038	0.036
25	0.00156	0.5	190∼1000	0.0382	0.034	0.030
35	0.000166	0.82	400∼4000	0.0315	0.027	0.019
45					0.022	0.012

[a] The molecular weight range over which the equation and constants are valid. [b] Intrinsic viscosity was calculated by the Mark−Houwink equation, $[\eta] = KM^a$ where molecular weight is 600. [c] Adapted from ref 33.

most serious problems of the PLGA-*g*-PEG system is the reconstitution the drug formulation after the freeze−drying process. Without any external additives, it takes several hours to dissolve the polymer with phosphate buffer. This might be improved by a decrease in hysteresis with added PEG because the hysteresis is associated with a dehydration−rehydration cycle.

To understand the phase behavior of the PLGA-*g*-PEG aqueous solution, intrinsic viscosity, FTIR, Raman, and SANS were studied as a function of temperature. The change in the hydrodynamic volume of the PEG with increasing temperature can provide useful information on the phase behavior of the PLGA-*g*-PEG aqueous solution.

Assuming the spherical model of a polymer, intrinsic viscosity is proportional to the hydrodynamic volume (V_h) of a chain (equation 3).[32]

$$V_h \sim [\eta]M \sim (4\pi R^3/3) \tag{3}$$

R and *M* are the equivalent hydrodynamic radius and molecular weight of a polymer chain. Therefore, the change in each block dimension with increasing temperature can be inferred from the study of intrinsic viscosity as a function of temperature. Both monomethoxy poly(ethylene glycol) MPEG (MW = 550, PDI = 1.02) and PEG (MW = 600, PDI = 1.02) were studied because the methoxy end group in PEG may affect the viscosity especially when the molecular weight of PEG is not high. In the PLGA-*g*-PEG copolymers, one side of the PEG (MW = 600) end groups is attached to the hydrophobic PLGA backbone. The solution behavior of PEG may be different when they are attached to the hydrophobic moiety. This might be inferred by comparing hydrodynamic radius of the PEG and the MPEG in water as a function of temperature. In the PEG with dihydroxyl terminal end groups, there are reference values of intrinsic viscosity as a function of temperature (Table 2). These values were also compared as references (Figure 7).[33] The intrinsic viscosity of the MPEG and the PEG decreased with increasing temperature. On the basis of eq 3, the relative hydrodynamic radii were compared in Figure 7 to the calculated value for the PEG 600 (PEG 600-calc) at 20 °C. One interesting finding was that the relative hydrodynamic radius of the MPEG decreased more rapidly over 20∼45 °C than the dihydroxy terminated PEG. This indicates that water becomes a poorer solvent for the MPEG than the PEG as the temperature increases, and it accelerates the dehydration of the MPEG with increasing temperature in a range of 20−45 °C.

IR Study. The IR spectra of the PLGA-*g*-PEG (PIII) aqueous solution (25 wt %) and a neat film were recorded as a function of temperature. The IR absorption peaks at 1757 and 1097 cm^{-1} are assigned to a carbonyl (C═O) stretching mode of the PLGA and an ether (C−O) bending mode of the PEG and the PLGA ester, respectively.[34] The IR spectrum of the PLGA-*g*-PEG aqueous solution exhibited no noticeable change around sol-to-gel transition temperature (about 30 °C) of the polymer in water (25 wt %). This indicates the microenvironment of the polymer is preserved during the sol-to-gel transition. At the gel-to-sol transition temperature, significant changes in IR absorption of carbonyl and ether groups were observed. On the other hand, there was no noticeable change in peak position and intensity for the neat polymer sample between 10 and 50 °C (Figure 8a and Figure 9).

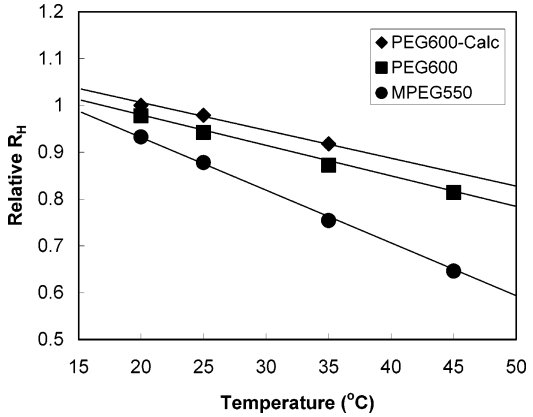

Figure 7. Change in hydrodynamic radius (R_H) of PEG 600-Calc, PEG (MW = 600, PDI = 1.07), and MPEG (MW = 550, PDI = 1.07) relative to that of calculated value of the PEG (PEG 600-Calc) at 20 °C as a function of temperature. Hydrodymanic radii of all above polymers in water decrease as the temperature increases.

The core (PLGA)−shell (PEG) was reported to be a basic structure of this material in water because it is composed of hydrophilic (PEG) and hydrophobic (PLGA) blocks based on ^{13}C NMR, Cryo-TEM, and hydrophobic dye solubilization.[14−16,20,35] There seems to be no hydrogen bonding between water and the ester groups of the PLGA below syneresis, indicating that the core PLGAs associate with themselves rather than exposed to water molecules. The core−shell structure, however, is broken at the gel-to-sol transition temperature by syneresis of the PLGA-*g*-PEG so that some of the PLGA is exposed to water and consequently hydrogen bonds to it. This hypothesis is also supported by a ^{13}C NMR study in D_2O.[20] In the sol state, at the sol-to-gel transition, and through the gel phase, the PEG appeared as a sharp peak, whereas the PLGA appeared as a collapsed and broadened peak in the ^{13}C NMR spectra, indicating core−shell structure of the system at these phases. Above the gel-to-sol transition temperature, the PLGA peak becomes sharp and increases in its intensity in the ^{13}C NMR spectrum. This reflects an increase in molecular motion, disruption of core−shell structure, and exposure of the core PLGA to aqueous environment. The exposed PLGA can more easily hydrogen bond to water than hidden PLGA inside the core of the core−shell structure. In comparison, the PLGA-*g*-PEG copolymer cast in the neat state without water exhibits a carbonyl peak that does not shift to lower frequency in the same temperature range. Therefore, the change in the carbonyl peak can be attributed to water−PLGA polymer interactions, suggesting that there is a disruption of the core−shell structure and

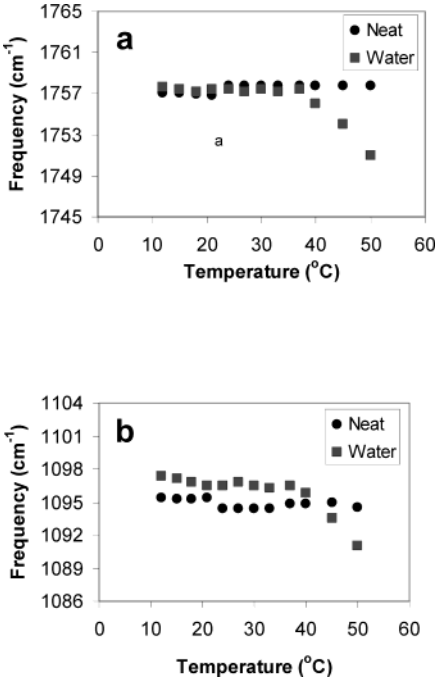

Figure 8. Change in peak position (gray square) of C═O stretching (a) and C−O bending (b) in the FTIR spectrum of the PLGA-*g*-PEG (PIII) aqueous solution (25 wt %) as a function of temperature. The peak positions of neat polymer film (filled circle) are compared as a reference in the same temperature range.

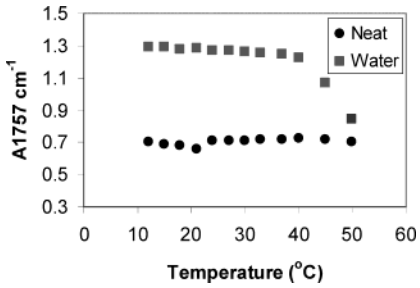

Figure 9. Change in absorbance at 1757 cm^{-1} (empty square) in FTIR spectra of the PLGA-*g*-PEG (PIII) aqueous solution (25 wt %) as a function of temperature. The absorbance of neat polymer (gray circle) is also compared as a reference in the same temperature range.

a subsequent exposure of PLGA to water above the syneresis temperature. Depending on the strength of hydrogen bonding, the shift in the carbonyl peak frequency varies from 6 to 100 cm^{-1}.[36,37] Below the lower critical solution temperature (LCST) of poly(N-isopropyl acrylamide) (PNIPAAm), the amide I peak was fitted with a single component centered at 1625 cm^{-1} whereas, above LCST, it was fitted with two components centered at 1625 and 1650 cm^{-1}. The peak at 1625 cm^{-1} was assigned to carbonyl groups hydrogen bonded to water and the peak at 1650 cm^{-1} was assigned to carbonyl groups hydrogen bonded to N−H in the polymer side chain.[38] Above the LCST, the hydrogen bonding between water and amide groups of polymers are disrupted and the carbonyl peak position increases by 25 cm^{-1}. Ascorbic palmitate potassium salt (APK) is a surfactant with core−shell structure in water. The solubility of the APK increases as the temperature increases.[39] The carbonyl peak at 1746 cm^{-1} (20 °C) shifted to 1731 cm^{-1} at 46 °C and to 1725 cm^{-1} at 56 °C. The carbonyl peak intensity of the APK also decreased with increasing temperature. They suggested that the change in the carbonyl peak is caused by an increase in hydrogen bonding because more exposure of carbonyl group to water occurs as the temperature increases.

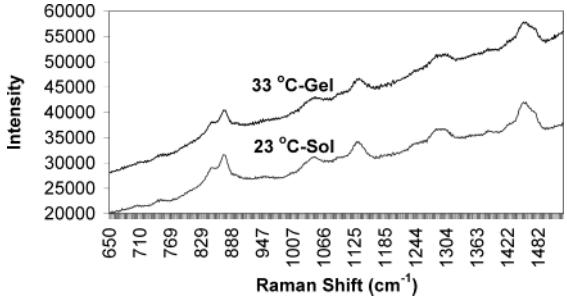

Figure 10. Comparison of Raman spectra of the PLGA-*g*-PEG (PIII) aqueous solution (25 wt %) in a sol (23 °C) and gel (33 °C) states. No change in peak position, but large increase in background scattering intensity suggests the micellar aggregates formation in the gel state.

The C−O bending mode around 1097 cm^{-1} shows a trend similar to that observed for the carbonyl peaks (Figure 8b). The C−O bending includes contributions from both the C−O bond of the ester (PLGA) and the C−O bond of the ether (PEG). The peak position does not change at the sol-to-gel transition temperature, indicating an insignificant change in hydration status. The IR spectra of a PLGA-*g*-PEG neat film were used as a reference. At the gel-to-sol transition temperature, involving syneresis, there was a shift in peak position from 1097 to 1091 cm^{-1}. However, there was no change in this peak for the neat film between 10 and 50 °C, suggesting that the change in the C−O bending mode also come from changes in the polymer−water interactions.

On the basis of the observation of intrinsic viscosity, IR spectra, and ^{13}C NMR data reported previously, the sol-to-gel transition and gel-to-sol transition appear to be caused by the dehydration of the PEG. The partial dehydration of the PEG at the sol-to-gel transition temperature keeps the core−shell structure during the sol-to-gel transition and through the gel phase, and this was not detected by IR spectroscopy. However, this partial dehydration of the PEG is strong enough to induce the micellar aggregation because the hydrophilicity and hydrophobicity of the thermogelling system is in balance. At the gel-to-sol transition temperature, significant dehydration of the PEG causes macrophase separation (syneresis) between water and the polymer. The core−shell structure is consequently broken and exposure of the PLGA to aqueous environment occurs. Such a change in hydration status is detected by IR spectroscopy and ^{13}C NMR.

Raman spectra of the PLGA-*g*-PEG (PIII) aqueous solution (25 wt %) exhibit vibration modes between 650 and 1500 cm^{-1} that are not strongly affected by the sol-to-gel transition (Figure 10). Peak positions, in particular, were not observed to change. Other regions of the Raman spectra behaved similarly. This result is consistent with the infrared spectra that showed no significant changes in the hydration status during sol-to-gel transition. On the other hand, the Raman spectra do show an increase in background intensity from 20 000∼35 000 to 30 000∼55 000 between 650 and 1500 cm^{-1} during the sol-to-gel transition. This is consistent with an increase in diffuse scattering from aggregates in the gel as they form. At higher temperature, the background scattering increases, supporting the micellar aggregation model for gelation. Unlike the infrared spectra, the Raman spectra could not be used to study changes at the syneresis temperature because the background had increased so significantly at this temperature that no further analysis of the spectra could be made.

SANS Study. SANS measurements were made at different temperatures to gain insight on the structural change induced by sol-to-gel transition. In Figure 11, results for a 20 wt % PEG-

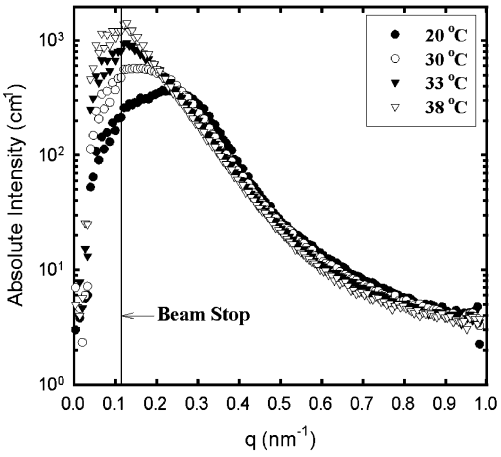

Figure 11. SANS profiles of a 20 wt % PLGA-*g*-PEG (PIII) aqueous solution as a function of temperature. Temperatures of the block copolymer aqueous solution are indicated in the legend. $\mathbf{q}_{max}$ shift from 0.25 to 0.15 suggests micellar aggregation during sol-to-gel transition.

g-PLGA (PIII) aqueous solution is presented in a semilogarithmic plot of scattered intensity as a function of scattering vectors **q**. The first peak originating from the micellar *d* spacing of about 29.2 nm is observed at 20 °C. With the increase in temperature up to 30 °C, the first scattering peak moves to a lower **q** value. The $\mathbf{q}_{max}$ values are shifted to even lower **q** values presumably because of the more extensive micelle clustering at 33 °C (gel state). With further increase in temperature, the overall SANS profiles do not change, suggesting that the PEG-*g*-PLGA (PIII) becomes a random aggregation of the micelles.

The results from the intrinsic viscosity, IR spectroscopy, Raman spectroscopy, and SANS studies provide important information on the sol-to-gel (lower transition) and gel-to-sol transition (upper transition) mechanism. First, the aggregation of micelles occurs at the sol-to-gel transition, which is sensitively detected by scattering methods, such as Raman spectroscopy and SANS. Such a nanoscopic change in aggregation of micelles leads to an abrupt increase in modulus and viscosity of the PLGA-*g*-PEG aqueous solution. However, the change in hydration status is not so significant, and the core−shell structure is preserved. Second, the significant changes in hydration state of the PLGA-*g*-PEG copolymer results in a gel-to-sol transition at higher temperature. Such a dehydration was sensitively detected by IR spectroscopy and macroscopic phase separation occurs at this temperature.

IV. Conclusions

The aqueous solution of the PLGA-*g*-PEG copolymers showed a sol-to-gel transition as the temperature increases. With further increase in temperature, the gel underwent a gel-to-sol transition with a macroscopic phase separation between water and polymers. The gel modulus and viscosity increased abruptly at the sol-to-gel transition and showed a maximum around the body temperature. The sol-to-gel transition temperature was controlled by varying the polymer composition and the number of the PEG graft. External PEGs as additives also changed the sol-to-gel transition temperature and the hysteresis loop between heating and cooling curves.

At the sol-to-gel transition, the PEG was partially dehydrated but kept the core−shell structure of the polymers. The partial dehydration of the PEG causes micellar aggregation which is detected by scattering experiments such as Raman and SANS. ^{13}C NMR and IR spectra show the presence of core−shell structure at this transition temperature.

In comparison, the dehydration of the PEG is so significant at the gel-to-sol transition temperature that the core−shell structure is broken and macroscopic phase separation occurs between water and the PLGA-*g*-PEG polymers. Such a significant change in hydration status was detected by the IR spectroscopy.

Acknowledgment. This work was supported by the Intramural Research Grant of Ewha Womans University, the Ministry of Science and Technology (MOST) of Korea, Korea Science and Engineering Foundation (KOSEF) (Grant RO1-2002-000-00274-0), and Battelle Independent Research & Development fund. Pacific Northwest National Laboratory is operated by Battelle Memorial Institute for the U.S. Department of Energy under contract DE-AC06-76RLO 1830.

References and Notes

(1) Galaev, I. Y.; Mattiasson, B. *Trends Biotechnol.* **1999**, *17*, 335−340.
(2) Lackey, C. A.; N. M.; Press, O. W.; Tirrell, D. A.; Hoffman, A. S.; Stayton, P. S. *Bioconjugate Chem.* **1999**, *10* (3), 401−405.
(3) Lim, Y. B.; Choi, Y. H.; Park, J. S. *J. Am. Chem. Soc.* **1999**, *121* (24), 5633−5639.
(4) Izumi, A.; Momura, R.; Masuda, T. *Macromolecules* **2001**, *32*, 4342−4347.
(5) Petka, W. A.; Harden, J. L.; McGrath, K. P.; Writz, D.; Tirrell, D. A. *Science* **1998**, *281*, 389−392.
(6) Wang, C.; Stewart, R. J.; Kopecek, J. *Nature* **1999**, *397*, 417−420.
(7) Jeong, B.; Lee, K. M.; Gutowska, A.; An, Y. H. *Biomacromolecules* **2002**, *3*, 865−868.
(8) Jeong, B.; Gutowska, A. *Trends Biotechnol.* **2002**, *20* (7), 305−311.
(9) Gutowska, A.; Jeong, B.; Jasionowski, M. *The Anatomical Record* **2001**, *263*, 342−349.
(10) Stile, R. A.; Burghardt, W. R.; Healy, K. E. *Macromolecules* **1999**, *32*, 7370−7379.
(11) Booth, C.; Attwood, D. *Macromol. Rapid Commun.* **2000**, *21*, 501−527.
(12) Malstom, M.; Lindman, B. *Macromolecules* **1992**, *25*, 5446−5450.
(13) Bromberg, L. *J. Phys. Chem. B* **1998**, *102*, 1956−1963.
(14) Jeong, B.; Bae, Y. H.; Kim, S. W. *Macromolecules* **1999**, *32*, 7064−7069.
(15) Jeong, B.; Kibbey, M. R.; Birnbaum, J. C.; Won, Y. Y.; Gutowska, A. *Macromolecules* **2000**, *33*, 8317−8322.
(16) Jeong, B.; Wang, L. Q.; Gutowska, A. *Chem. Commun.* **2001**, *16*, 1516−1517.
(17) Behravesh, E.; Shung, A. K.; Jo, S.; Mikos, G. *Biomacromolecules 3*, 153−158.
(18) Chenite, A.; Chaput, C.; Wang, D.; Combes, C.; Buschmann, M. D.; Hoemann, C. D.; Leroux, J. C.; Atkinson, B. L.; Binette, F.; Selmani, A. *Biomaterials* **2000**, *21*, 2155−2161.
(19) Lee, B. H.; Lee, Y. M.; Sohn, Y. S.; Song, S. C. *Macromolecules* **2002**, *35*, 3876−3879.
(20) Chung, Y. M.; Simmons, K.; Gutowska, A.; Jeong, B. *Biomacromolecules* **2002**, *3*, 511−516.
(21) Harris, J. M. *Poly(ethylene glycol) Chemistry*; Plenum Press: New York, 1993; pp 263−268.
(22) Cho, K.; Kim, C. H.; Lee, J. W.; Park, J. K. *Macromol. Rapid Commun*. **1999**, *20*, 598−601.
(23) Wyatt, P. J. *Anal. Chim. Acta* **1993**, *272*, 1−46.
(24) Tanodekaew, S.; Godward, J.; Heatley, F.; Booth, C. *Macromol. Chem. Phys*. **1997**, *198*, 3385−3395.
(25) Gilbert, J. C.; Richardson, J. L.; Davies, M. C.; Palin, K. J.; Hadgraft, J. *J. Controlled Release* **1987**, *5*, 113−118.
(26) Wanka, G.; Hoffmann, H.; Ulbricht, W. *Colloid Polym. Sci*. **1990**, *268*, 101−117.
(27) Pawer, R. J. M.S. Thesis, University of Utah, 1995, pp 13−20.
(28) Jeong, B.; Lee, D. S.; Shon, J. I.; Bae, Y. H.; Kim, S. W. *J. Polym. Sci. Polym. Chem*. **1999**, *37*, 751−760.
(29) Sepe, M. P. *Polymer handbook series: Dynamic mechanical analysis for plastics engineering, Plastic design library*; New York, 1998; pp 1−29.
(30) Wong, J. Y.; Velasco, A.; Rajagopalan, P.; Pham, Q. *Langmuir* **2003**, *19*, 1908−1913.

(31) Lo, C. M.; Qang, H. B.; Dembo, M.; Qang, Y. L. *Biophys. J.* **2000**, *79*, 144−151.
(32) Zhou, Z.; Chu, B. *Macromolecules* **1984**, *27*, 2025−2033.
(33) Brandrup, J.; Immergut, E. H. *Polymer Handbook*, 2nd ed.; John Wiley & Sons: New York, 1975; pp IV−23.
(34) Zhu, Z.; Xiong, C.; Zhang, L.; Yuan, M.; Deng, X. *Eur. Polym. J.* **1999**, *35*, 1821−1828.
(35) Jeong, B.; Bae, Y. H.; Kim, S. W. *Colloids Surf., B* **1999**, *16*, 185−193.
(36) Lambert, J. B.; Shurvell, H. F.; Verbit, L.; Cook, R. G.; Stout, G. H. *Organic structural analysis*; Macmillan Publishing Co., Inc.: New York, 1976; p 294.
(37) Maegda, Y.; Higuchi, T.; Ikeda, I. *Langmuir* **2000**, *16*, 7503−7509.
(38) Maegda, Y.; Higuchi, T.; Ikeda, I. *Macromolecules* **2001**, *34*, 1391−1399.
(39) Griffiths, P. R.; Haseth, J. A. *Fourier Transform Infrared Spectrometry*; John Wiley & Sons: New York, 1986; pp 464−465.